Neural Computing and Applications
https://doi.org/10.1007/s00521-024-10552-0

S.I.: TIMELY ADVANCES OF DEEP LEARNING WITH APPLICATIONS AND DATA DRIVEN MODELING

Conditioned fully convolutional denoising autoencoder for multi-target NILM

Diego García[1] · Daniel Pérez[2] · Panagiotis Papapetrou[3] · Ignacio Díaz[1] · Abel A. Cuadrado[1] · José M. Enguita[1] · Manuel Domínguez[2]

Received: 15 December 2023 / Accepted: 3 October 2024

Abstract
Energy management requires reliable tools to support decisions aimed at optimising consumption. Advances in data-driven models provide techniques like Non-Intrusive Load Monitoring (NILM), which estimates the energy demand of appliances from total consumption. Common single-target NILM approaches perform energy disaggregation by using separate learned models for each device. However, the use of single-target systems in real scenarios is computationally expensive and can obscure the interpretation of the resulting feedback. This study assesses a conditioned deep neural network built upon a Fully Convolutional Denoising AutoEncoder (FCNdAE) as multi-target NILM model. The network performs multiple disaggregations using a conditioning input that allows the specification of the target appliance. Experiments compare this approach with several single-target and multi-target models using public residential data from households and non-residential data from a hospital facility. Results show that the multi-target FCNdAE model enhances the disaggregation accuracy compared to previous models, particularly in non-residential data, and improves computational efficiency by reducing the number of trainable weights below 2 million and inference time below 0.25 s for several sequence lengths. Furthermore, the conditioning input helps the user to interpret the model and gain insight into its internal behaviour when predicting the energy demand of different appliances.

Keywords Non-intrusive Load Monitoring · Energy Efficiency · Deep Convolutional Neural Networks · Interpretability · Multi-target NILM models

✉ Diego García
garciaperdiego@uniovi.es

Daniel Pérez
dperl@unileon.es

Panagiotis Papapetrou
panagiotis@dsv.su.se

Ignacio Díaz
idiaz@uniovi.es

Abel A. Cuadrado
cuadradoabel@uniovi.es

José M. Enguita
jmenguita@uniovi.es

Manuel Domínguez
manuel.dominguez@unileon.es

[1] Department of Electrical Engineering, University of Oviedo, Gijón 33209, Principado de Asturias, Spain

[2] SUPPRESS Research Group, University of León, León 24007, Spain

[3] Department of Computer and Systems Science, Stockholm University, Kista, SE-164 07, Stockholm, Sweden

Published online: 05 December 2024

1 Introduction

Energy efficiency has gained significant attention, not only in the promotion of sustainable products and generation technologies aimed at saving energy, but also in the study of current systems to obtain knowledge about energy consumption patterns. Frequently, this consumption is reported as an overview of the total demand in a certain period of time which can enhance users' energy awareness. However, detailed representations of energy consumption help users to obtain further feedback, prompting them to take specific actions to improve overall energy efficiency [14, 18].

This growing interest in detailed energy representations has led to the development of energy disaggregation techniques, commonly known as *Non-Intrusive Load Monitoring* (NILM) [4, 15, 46, 54]. NILM analysis decomposes the energy consumption of a facility by estimating the appliance-specific loads using only measurements from the main energy demand. Unlike other intrusive methods, NILM provides energy disaggregation using only data collected from the main meter, reducing cost and complexity.

NILM disaggregation addresses the problem of estimating diverse appliance load signatures across various facilities. The load signature of devices can be grouped into categories, such as systems with two states of operation (ON/OFF), with a finite number of operating states, or permanent consumer devices that remain active all the time [4]. Moreover, energy consumption patterns are influenced by the type of the facility. For example, residential facilities include common household appliances; while, non-residential large buildings, such as educational campuses, hospitals or factories, integrate different types of devices and subsystems (thermal comfort systems, lifts, etc.) with distinct energy demand patterns.

All these complexities have been addressed using data-driven nonlinear models [4, 30] in order to achieve a reliable energy disaggregation. *Machine Learning* techniques, for instance, are commonly applied to classify appliance operating states or predict energy consumption of each device from aggregated data. *Deep Neural Networks* (DNN) [36] have demonstrated superior accuracy compared to earlier machine learning models in the NILM problem, making significant advancements in this field [31, 42]. DNN-based approaches constitute the foundation of current research and improvements in NILM. Typical DNN architectures include *Convolutional Neural Networks* (CNN) [40] applied to time series, such as 1D CNN [16], *denoising AutoEncoders* (dAEs) [7, 21, 31], or *Recurrent Neural Networks* (RNN) focussed on temporal dependencies [29].

Currently, the majority of DNN-based NILM models consist of a set of trained networks for each individual consumption independently. This means that a *single-target* network is dedicated to estimating the energy consumption of a specific appliance. Thus, the resources of these models for full disaggregation in a facility involve high computational costs. As an alternative to single-target NILM models, *multi-target* disaggregation allows the estimation of all individual appliances from the main energy consumption by training only one neural network [16, 30]. Generally, the estimation of all appliances is achieved by increasing the number of outputs and the depth of the DNN architectures, resulting in more complex models, since the number of trainable weights and the time needed to estimate each individual consumption increase significantly.

Although multi-target models have demonstrated comparable performance to single-target methods [16, 20], they are still under development and require further exploration of relevant aspects in the NILM field. The main research on multi-target models focuses on the accuracy of the disaggregation for residential facilities. However, other key aspects essential for the deployment of NILM systems, such as computational efficiency, transferability to diverse facility types, and interpretability, have been frequently overlooked in prior analyses. These factors are particularly important in providing actionable feedback to the user and would help end users to gain understanding of energy demand and confidence in the model.

A new perspective of multi-target NILM models, called multi-FCNdAE, was introduced in [20]. The model is built upon a single-output *Fully Convolutional denoising Auto-Encoder* (FCNdAE) [21], incorporating a conditioning input to specify the target appliance. Based on this approach, this article extends the assessment of the multi-FCNdAE model to several domains. The contributions of this work include:

- Evaluation of the model performance against single-target and multi-target methods using established NILM metrics.
- The use of both residential and non-residential data to broaden applicability.
- Computational efficiency through trainable weights and time to obtain output.
- Exploration of conditioning mechanisms to enhance the model interpretability.

To sum up, this work advances the study of the multi-FCNdAE model, extending its application in various scenarios, improving accuracy and efficiency in energy consumption disaggregation. Furthermore, the use of a conditioning input helps to interpret and understand the model with practical utility.

The remainder of the paper is organised as follows. In Sect. 2, a brief revision of related work is presented. In Sects. 3.1 and 3.2, the single-target and multi-target NILM perspectives are detailed, respectively. The proposed multi-FCNdAE is defined in Sect. 3.3. All the experimental considerations are detailed in Sect. 4. In Sect. 5, the performance, computational efficiency, and interpretability of the proposed method are evaluated. Finally, the conclusions and future work are presented in Sect. 6.

2 Related work

Numerous works related to energy disaggregation have been reviewed by the research community [4, 15, 22, 46, 54], ranging from the description of the NILM problem to more practical and reliable approaches [30]. Other publications in the literature focus on specific aspects such as NILM datasets [27, 32] or performance evaluation [44].

Hart [24] defined a signature-based approach that focussed on finding transitions between steady-states on total consumption. This approach involves *combinatorial optimization* to find the best combination of available signatures that independently estimate disaggregation, without considering the temporal context. In contrast to the computationally expensive combinatorial approaches, *pattern recognition* methods rely on functions that efficiently map features extracted from the total energy consumption to the state of the appliances. Traditional *machine learning* techniques are also suitable for pattern recognition in NILM, especially supervised approaches, such as event detectors and appliances' state classifiers [3, 17, 37]. Other unsupervised techniques based on *Factorial Hidden Markov Models* (FHMM) [33, 34] have been explored to avoid the use of labelled data. FHMM achieved acceptable results, but suffered from limitations in computing models for several appliances with multiple operating states.

Deep neural networks have improved the performance of NILM models [26, 31, 42] and avoid the extraction of handcrafted features on the main consumption through the use of different *Deep Learning* (DL) architectures, such as *Recurrent Neural Networks* (RNN), *AutoEncoders* (AE) or *Convolutional Neural Networks* (CNN). RNNs are well-suited for modelling time series data due to their ability to maintain internal memory or state. By processing prior inputs to compute the internal state, RNNs effectively influence both the current input and output, enabling robust sequential data analysis. RNNs encompass various variants such as Gated Recurrent Units (GRU) or Long Short-Term Memory (LSTM) networks, which have been compared for energy disaggregation in [35]. The comparison revealed that GRU networks are more suitable for NILM due to the difficulty in training LSTM layers.

CNN models [2, 8] are popular in deep learning applications and consist of a sequence of convolution, pooling, normalisation and fully connected layers. CNNs efficiently exploit the temporal coherence in time series data by employing convolutional filters with a reduced number of trainable weights. This results in smaller architectures that are less complex, yet highly effective, with improved generalisation capabilities. In [51], authors proposed a deep CNN for predicting an instantaneous individual consumption from an input sequence of main consumption, leading to a sequence-to-point method that advances on previous sequence-to-sequence approaches.

In addition to vanilla CNN models, a wide variety of CNN-based architectures have also been developed. In [52], two inputs consisting of a differential and an auxiliary signal were used to generate the final sequence. In addition, two sub-networks in NILM models perform multiple tasks combining regression and classification [47], and also for the construction of a scale and context-aware network based on convolutional branches connected to a gating mechanism [10]. A modification of WaveNet [43], called WaveNILM, was proposed in [23], based on dilated causal convolutions achieving higher performance than previous methods.

In contrast to these approaches, NILM can also be treated as a noise reduction problem, where a *denoising AutoEncoder* (dAE) [31] is used to extract the corresponding appliance signal from the aggregated noisy signal [7]. This approach shows an improvement in both seen and unseen scenarios for household data and offers a certain degree of robustness against noise. A NILM system composed by a fully convolutional dAE (FCNdAE) was evaluated using real data from a hospital in [21], showing accurate estimations for short and long-term consumption.

Most DL-based models use one neural network per appliance for disaggregation. In contrast to this single-target approach, multi-target NILM models use a unique model to disaggregate all the individual appliances. The multi-target perspective contributes to the computational efficiency of the NILM models by reducing the complexity of the approach. A multi-task NILM model based on U-Net architecture has been proposed in [16] with a multi-label learning for state detection and multi-target quantile regression for power estimation. Another multi-target NILM, which is the baseline for this study, was presented in [20]. The authors proposed in this paper a FCNdAE network to estimate individual consumptions using a conditioning input that modulates intermediate activations for each specific appliance. While preliminary results in multi-target NILM have been reported, the challenge remains in developing efficient and accurate multi-target models that

provides interpretable and actionable feedback to the user, while maintaining comparable or superior accuracy compared to single-target models across various scenarios.

Previous works on NILM have focussed on approaches trained and evaluated on residential facilities. However, improvements in technology have led to the widespread installation of smart meters in buildings, enabling data collection in a broad range of facilities. Although there are a few works that evaluate non-residential buildings [21] and industrial energy consumption data [28], further efforts are required to assess NILM models in these increasingly common facilities.

Another important aspect of the NILM models is the interpretation of their outcome, since it facilitates users to improve the overall efficiency thanks to the knowledge gained from NILM feedback [5, 53]. In this sense, several solutions have emerged allowing the user to interact with the outcome of NILM models in interactive data visualisations [1, 19, 48]. Furthermore, improving the interpretability of NILM models would increase the level of confidence in their feedback [41], so any effort to improve transparency is valuable [6].

3 Methods

3.1 NILM problem formulation

NILM can be addressed as either a classification or a regression problem [30]. NILM as a classification problem involves predicting the operating states of downstream devices; whereas, the appliance-specific energy demand can be estimated directly through NILM regression models. This article only considers NILM as a regression problem due to its better scalability to non-residential domains, where labelling the states of each individual node could be challenging.

The outcome of NILM regression models is computed from a whole-facility energy consumption sequence, commonly denoted as $\mathbf{P}$. This sequence is the sum of all appliance-specific loads in the facility:

$$\mathbf{P} = \sum_{m=1}^{N} \mathbf{p}_m + \epsilon \tag{1}$$

where $\mathbf{p}_m$ represents a sequence —with the same length as $\mathbf{P}$— of the m-th individual load, ϵ represents an additive noise term, and N is equal to the number of individual consumptions of the facility. An *energy disaggregator* D_m is a function that extracts the m-th individual energy consumption from $\mathbf{P}$:

$$D_m : \mathbf{P} \rightarrow \hat{\mathbf{p}}_m \tag{2}$$

Most approaches follow the *single-target* strategy shown in Fig. 1a, where the individual consumptions are estimated by a set of N disaggregators $\{D_m\} \quad m = 1, 2, \ldots, N$. Single-target models are usually based on a previous *windowing operation*, which divides the whole sequence of total energy consumption (daily/monthly sequence) into smaller input sequences. This operation is defined by the window length L and the stride M between contiguous windows.

Once the windowing operation is applied, the resulting training windows of total and individual consumption $\{\mathbf{P}^{(i)}, \mathbf{p}_m^{(i)}\}$ are used to minimise the reconstruction loss function $\mathcal{L}$ in order to optimise the parameters θ, which defines the regression data-driven model D_m:

$$\begin{aligned} \theta^* &= \arg\min_{\theta} \frac{1}{n} \sum_{i=1}^{n} \mathcal{L}\left(\mathbf{p}_m^{(i)}, D_m(\mathbf{P}^{(i)}, \theta)\right) \\ &= \arg\min_{\theta} \frac{1}{n} \sum_{i=1}^{n} \mathcal{L}\left(\mathbf{p}_m^{(i)}, \hat{\mathbf{p}}_m^{(i)}\right) \end{aligned} \tag{3}$$

where $\hat{\mathbf{p}}_m^{(i)}$ is the estimated individual consumption sequence for the i-th training sample and θ^* the optimised weights. Reconstruction error functions, such as *Root Mean Squared Error* (RMSE) or *Mean Squared Error* (MSE), are often used as loss functions in DNN-based NILM models.

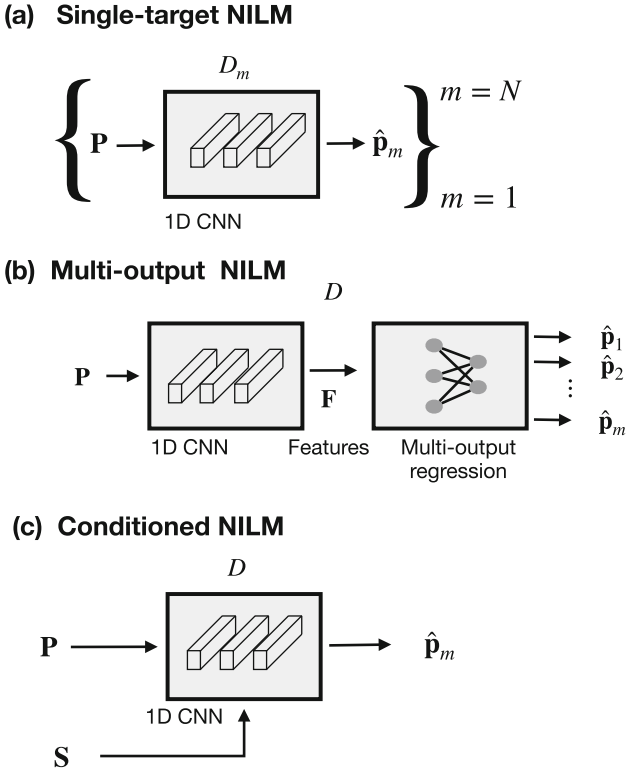

Fig. 1 Different approaches for NILM. From top to bottom: **a** single-target, **b** multi-output and **c** conditioned multi-target NILM approaches

After training, each disaggregator D_m estimates an individual sequence $\hat{\mathbf{p}}_m$ from a sequence of total consumption $\mathbf{P}$. In practice, this approach entails excessive memory usage in the analysis because a total of N models must be loaded and executed to obtain all individual consumptions. In addition, it is not easy to interact with the model beyond varying the input sequence. In Sect. 2, several models were mentioned [7, 10, 21, 29] as suitable energy disaggregation functions D_m.

3.2 Multi-target NILM

In contrast to the single-target NILM formulation above, in multi-target NILM only one disaggregator D is trained:

$$D : \mathbf{P} \rightarrow \hat{\mathbf{p}} \tag{4}$$

The output of the D model consists of a set of N estimations, one per appliance, denoted as $\hat{\mathbf{p}} = [\hat{\mathbf{p}}_1, \hat{\mathbf{p}}_2, \ldots, \hat{\mathbf{p}}_N]$. Recent multi-target approaches have proposed variants of previous single-target DNN models [9, 16, 50]. They typically consist of a feature extraction stage, which can be a 1D CNN [16, 50], or a feature selection method [9], followed by a multi-target regression or classifier. A shallow fully connected neural network, which maps the learned features to the output, is used as a multi-target stage in [16, 50]. This multi-output approach is graphically represented in Fig. 1b. This results in a significant increase in the number of weights, especially for large numbers of extracted features $\mathbf{F}$ and appliances N to be disaggregated. This leads to greater memory requirements for storing and running the model, an increasing risk of overfitting, and restricted scalability to facilities with varying numbers of appliances.

In Fig. 1c, a representation of the alternative conditioned multi-target NILM perspective presented in [20] is also included. Instead of varying the output, an auxiliary input, denoted as *conditioning input* $\mathbf{S}$, is incorporated into a single-target model. A conditioning mechanism processes $\mathbf{S}$ and modulates the intermediate activations of the CNN layer in order to prepare the overall model to estimate the targeted appliance $\hat{\mathbf{p}}_m$.

This approach could mitigate previously mentioned limitations of the multi-output models and provide users with an interactive pathway to steer the DNN model, potentially paving the way for more flexible and interpretable multi-target NILM models. The conditioned multi-target NILM, the conditioning mechanism, and the multi-FCNdAE architecture are further explained in the following section.

3.3 Conditioned multi-FCNdAE

Conditioned DNN models, such as the conditioned NILM model suggested in Fig. 1c, have recently been studied in other application areas, with a focus on modulating the intermediate activations of the main network using the auxiliary input $\mathbf{S}$. These modulations are commonly performed by simple functions such as *biasing* [39], *scaling* [11, 25] or *affine* [12, 13] transformations. *Feature-wise Linear Modulation* (FiLM) [45] is a general-purpose conditioning framework based on applying affine transformations to the output of the intermediate convolution layers of a CNN using the FiLM layer shown in Fig 2 and defined as:

$$\mathrm{FiLM}(\mathbf{F}_{j,k}^{(i)}, \gamma_{j,k}, \beta_{j,k}) = \mathbf{F}_{j,k}^{(i)}\gamma_{j,k} + \beta_{j,k} \tag{5}$$

where the k-th channel of the output feature map from the j-th convolution layer $\mathbf{F}_{j,k}^{(i)}$ is element-wise scaled by $\gamma_{j,k}$ and shifted by $\beta_{j,k}$. Note that the FiLM operation only introduces two parameters per channel to be conditioned, so that they are independent of the size of the input sequence to the network.

The FiLM framework modulates the output of the network by stacking FiLM layers between convolution layers. All γ and β required by the stacked FiLM layers are computed from the conditioning input $\mathbf{S}$ by the *FiLM generator* $\mathbf{g}$:

$$\{\gamma, \beta\} = \mathbf{g}(\mathbf{S}) \tag{6}$$

In practice, the FiLM generator $\mathbf{g}$ is implemented as an auxiliary neural network with two outputs, which takes as input the selection of the individual consumption to be disaggregated. For the sake of simplicity, in the rest of the article we refer to $\mathbf{S}_m$ when the m-th individual consumption is selected for disaggregation.

The FiLM framework is used to transform the single-target FCNdAE model [21] into the multi-FCNdAE model [20], displayed in Fig. 3. Once the $\mathbf{S}$ is introduced in the model, all the FiLM parameters $\{\gamma, \beta\}$ are computed by a FiLM generator made of three fully connected layers.

The computed FiLM parameters are then used to modulate the encoder in the main network. The encoder in Fig. 3 encompasses two convolution blocks. Each convolution block consists of two consecutive convolution layers with stride of 1, followed by another convolution layer with a stride of 2, reducing the input sequence size L by half. All the convolution layers in the encoder are modulated by FiLM layers. The output of the convolution blocks is then compressed to a sequence of q elements by a convolution layer with a kernel size of $L/4$ and q number of kernels. By modulating only the encoder, the latent space representation $\mathbf{z}^{(i)}$ is conditioned on the target consumption indicated

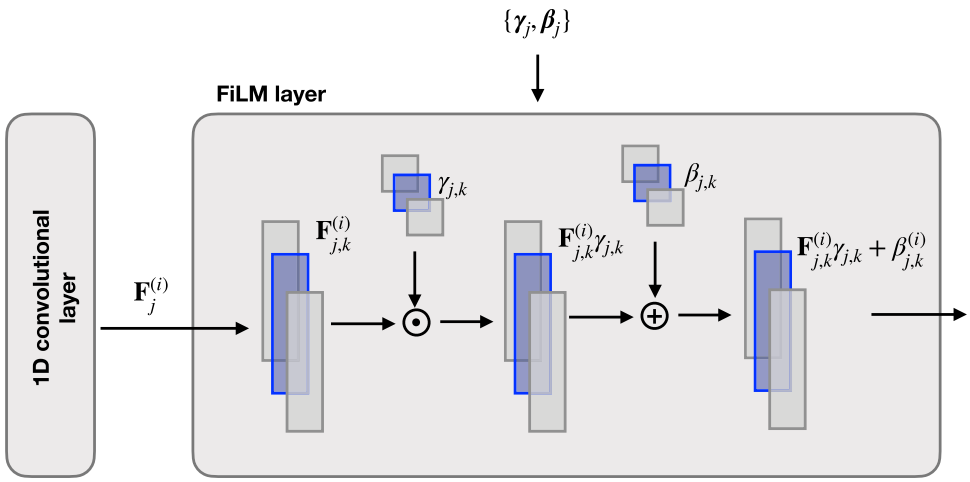

Fig. 2 Representation of the affine transformation inside of a FiLM layer. The affine transformation is illustrated for the k-th channel (blue) of the j-th convolution layer output $\mathbf{F}_j$

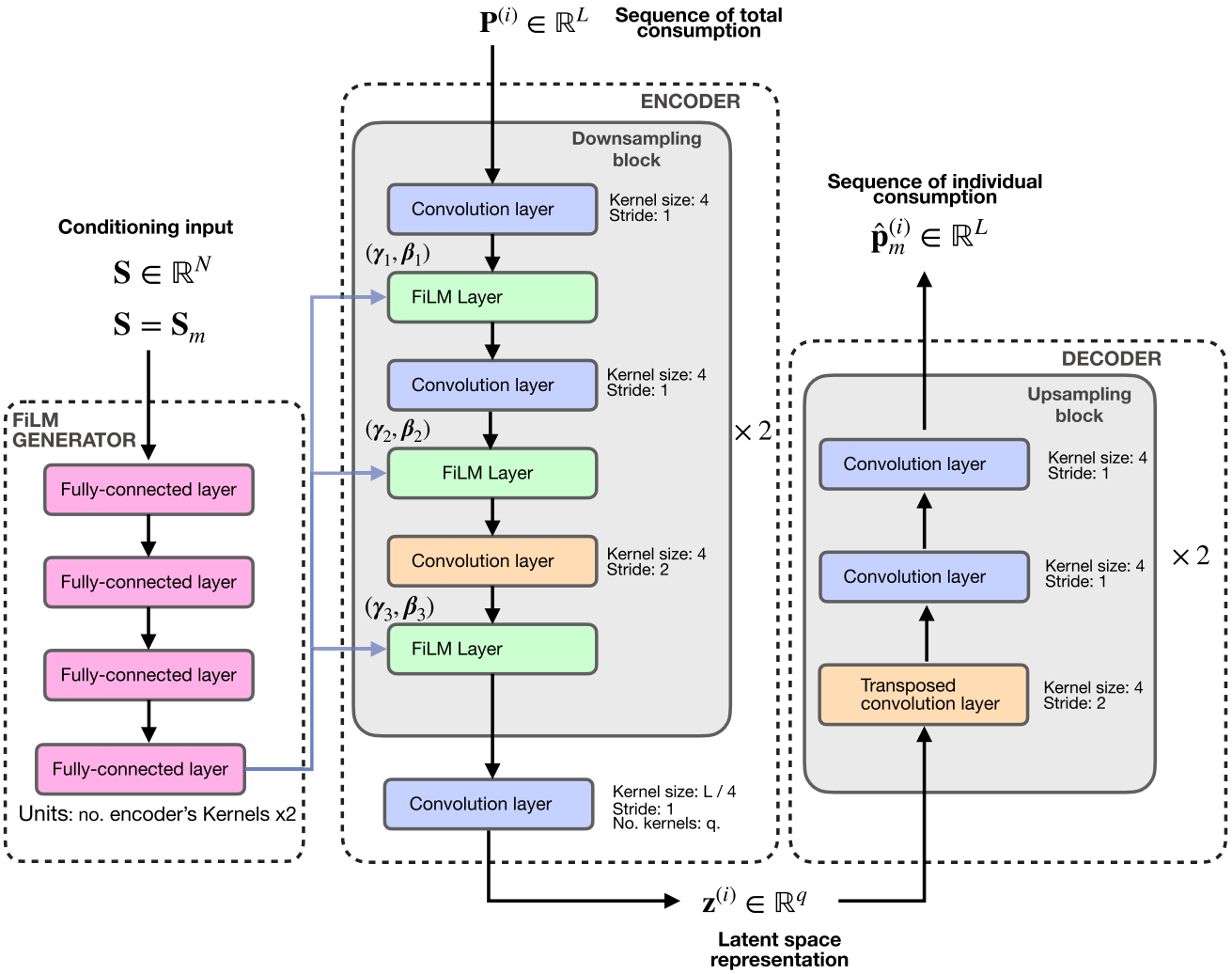

Fig. 3 Architecture of the proposed conditioned multi-FCNdAE architecture

in $\mathbf{S}$, so that it contains distinct regions based on the selected individual consumptions.

Finally, the decoder upsamples $\mathbf{z}^{(i)}$ to the estimated individual consumption $\hat{\mathbf{p}}_m^{(i)}$ using two convolution blocks

consisting of a transposed convolution layer with a stride of 2 and two subsequent convolution layers with a stride of 1.

The targeted individual consumptions are indicated in $\mathbf{S}$ as a one-hot encoding vector, denoted as $\mathbf{S}_m$. However, more complex formats of $\mathbf{S}_m$, such as attributes related to the individual consumption (e.g. location, type of consumption or any prior knowledge) are also appropriate.

4 Experimental set-up

Data. The UK-DALE residential dataset [32] and a hospital complex dataset [21] are used to evaluate the proposed model. Thus, the analysis encompasses both residential and non-residential contexts.

The UK-DALE dataset contains 1/6 Hz appliance-level and 1 Hz main-level energy consumptions records in 5 households over a span of more than four years. To unify the data, the overall sample rate is set to 1/6 Hz by downsampling the main energy consumption data. Data from *House* 1 are used to train and test the models. A year of data is reserved for training and four months for testing. Only data from fridge (FZ), kettle (KT), dishwasher (DW), washing machine (WM) and microwave (MW) are considered, as these appliances are the most common and representative of a household. The noise present in the selected individual consumptions is reduced by a median filter [16].

The non-residential dataset was recorded from a hospital complex [21], where the total energy consumption was measured together with 9 individual consumptions at a sampling rate of 1/60 Hz over one year, resulting in a total of 507353 samples. The individual nodes monitored are described in Table 1. They represent a comprehensive set of typical energy profiles within a hospital: lifts, diagnostic equipment, inpatient rooms and data processing servers. Duplicate nodes have been eliminated from the results presented in Sect. 5, refining the analysis to focus solely on the consumption of specific nodes: CGBT-2.Montante0 (lifts), Radiologia1 (X-ray), RehabilitacionA (rehabilitation), CPD (data centre), Plantas 2-7 (floors). In the case of the hospital data, ten months of data are used for model training and one month for model evaluation.

Training set-up. The models were trained using pairs of sequences of total and individual consumption, denoted as $\{\mathbf{P}^{(i)}, \mathbf{p}_m^{(i)}\}$. The training sequences are normalised using z-score normalisation. In order to train the multi-FCNdAE architecture, the one-hot vectors $\mathbf{S}_m$ are added to the training sequences. The models are trained using the Adam optimiser with a stepsize $\alpha = 0.001$, decay rate $\beta = 0.9$ and a batch size of 128. To mitigate overfitting, early stopping regularisation is implemented by monitoring the validation error during training epochs. The user-defined hyperparameters related to the main architecture and training process of the multi-FCNdAE model in Fig. 3 are detailed in Table 2. Regarding the computational resources, a computer with Debian GNU/Linux OS and equipped with a RTX 3090 Nvidia GPU card was employed to develop, train and evaluate all the models.

Metrics. *Root Mean Squared Error* (RMSE), *Mean Absolute Error* (MAE) and *Estimated Accuracy* (EAC) error metrics, commonly employed in NILM literature [4, 46] for regression methods, are applied to assess the models under study. These metrics are separately applied to the sequences of estimated individual consumptions $\hat{\mathbf{p}}_m$ of length T obtained from a main consumption $\mathbf{P}$ of the same length. RMSE_m measures the standard deviation of the energy estimation of the m-th individual consumption:

Table 1 Description of the individual nodes measured from the hospital facility

Meter	Description
Total consumption	Consumptions of whole facility
CGBT-2.Montante0	South zone lifts
Radiologia1	X-ray room 1
Radiologia2	X-ray room 2
RehabilitacionA	Rehab facilities A
RehabilitacionB	Rehab facilities B
Subcentral3	West zone consumption
CPD	Server and a data centre
Plantas_2-7	South zone floors from 2 to 7
Plantas_8-13	South zone floors from 8 to 13

Table 2 Hyperparameters of the multi-FCNdAE model illustrated in Fig. 3 for the two datasets employed in the experiments

	UK-DALE	HOSPITAL
Input length (L)	500	1440
No. epochs	100	100
Batch size	128	128
Early stopping	yes	yes
Early stopping patience	10	10
No. downsampling blocks	2	2
No. upsampling blocks	2	2
Kernel size	4	4
No. channels downsampling	(32, 64)	(32, 64)
No. channels upsampling	(64, 32)	(64, 32)
No. channels latent space (q)	26	26
No. neurons in FiLM Gen. layers	(32,32,32)	(32,32,32)

$$\mathrm{RMSE}_m = \sqrt{\sum_{t=1}^{T} \frac{(p_m(t) - \hat{p}_m(t))^2}{T}} \tag{7}$$

MAE_m measures the error in the estimated value of an individual energy consumption m at each time step:

$$\mathrm{MAE}_m = \frac{1}{T} \sum_{t=1}^{T} |p_m(t) - \hat{p}_m(t)| \tag{8}$$

while EAC_m reports a score value of accuracy for the disaggregation of individual consumption m:

$$\mathrm{EAC}_m = 1 - \frac{\sum_{t=1}^{T} |p_m(t) - \hat{p}_m(t)|}{2 \sum_{t=1}^{T} p_m(t)} \tag{9}$$

EAC_m is normalised by the total energy consumed by the individual consumptions, allowing for the comparison of individual estimations between each other.

5 Results and discussion

This section evaluates and discusses the accuracy, computational efficiency, and interpretability of the multi-FCNdAE model. The accuracy of the multi-FCNdAE is assessed against the single-target *denoising AutoEncoder* (dAE) [31], *biLSTM* [29] and vanilla FCNdAE [21] models. The *U-Net* approach proposed in [16] is also included to compare our model with a state-of-the-art multi-target approach. In Sect. 5.1, the UK-DALE dataset is utilised to evaluate the effectiveness in a residential domain, whereas, in Sect. 5.2, the models are evaluated in a non-residential scenario using data from the hospital described in Sect. 4. Computational efficiency, focussing on the number of weights and the models inference time, is addressed in Sect. 5.3. Finally, the potential benefits of multi-FCNdAE in terms of interpretability are discussed in Sect. 5.4.

5.1 Performance in residential data

The accuracy of multi-FCNdAE with respect to the aforementioned competitors for the UK-DALE dataset is shown in Table 3. Both FCNdAE-based approaches outperform the dAE and biLSTM models. This confirms that the FCNdAE architecture is a reliable baseline method to be expanded as a multi-target model. The FCNdAE approach shows slightly better MAE and EAC values compared to the multi-FCNdAE model, with higher accuracy in three of the five appliances analysed. Note that each individual model D_m in the FCNdAE approach is specifically trained to disaggregate one appliance, a simpler task than predicting all the appliances at once, as the multi-FCNdAE model does.

Figure 4 illustrates appliance-specific energy loads predicted by the models. The disaggregations align with the results presented in Table 3. The FCNdAE model shows consistent performance for all individual consumption time series, regardless of their nature. The multi-FCNdAE model gives similar results, but with offset errors for the washing machine and microwave appliances.

When the multi-FCNdAE approach is compared with the multi-target U-Net model in Table 3, it shows better MAE and EAC values for all appliances. Multi-FCNdAE exhibits greater consistency than the U-Net model for all the devices, as illustrated in Fig. 4.

5.2 Performance in non-residential data

Table 4 presents the MAE and EAC results for the multi-FCNdAE approach and its competitors when applied to the hospital data. Multi-FCNdAE and single-target FCNdAE architectures exhibit better overall metrics compared to the biLSTM and dAE models. The multi-FCNdAE model slightly improves the results of FCNdAE. In the individual energy loads predicted by the models depicted in Fig. 5, it can be observed that the FCNdAE model cannot reproduce short-term patterns, especially for *X-ray* node. This contributes to its loss of accuracy when compared to the multi-FCNdAE.

The multi-FCNdAE model displays better performance than the U-Net model for all individual consumptions. Comparing examples of estimated sequences of individual nodes in Fig. 5, the U-Net model performs better in reproducing short-term patterns but tends to introduce noise into the estimated sequences. Conversely, multi-FCNdAE demonstrates a smoother behaviour for all estimated individual nodes.

5.3 Computational efficiency

This section compares the computational efficiency by examining the number of trainable weights and the time required to obtain the output sequences of individual consumptions from a sequence of main consumption for each NILM model. The number of weights and inference time are significantly influenced by the input length L of the models. The optimal input length is a user-defined hyperparameter that depends on the data sampling rate, the model employed and the appliances or consumptions being estimated. In order to consider the effect of L on the computational efficiency evaluation, the inference time and number of weights, displayed in Fig. 6, are calculated for models with L values of 100, 500 and 1440 timesteps.

Table 3 MAE and EAC metrics of the dAE, biLSTM, FCNdAE, multi-target U-Net and *multi-FCNdAE* approaches for the dishwasher (DW), fridge (FZ), kettle (KT), microwave (MW) and washing machine (WM) appliances of UK-DALE dataset

		DW	FZ	KT	MW	WM
MAE	dAE	25.039	8.795	7.766	4.446	30.428
	biLSTM	23.805	3.940	12.973	4.713	11.687
	FCNdAE	6.451	**3.927**	3.804	**2.495**	**3.706**
	U-Net	16.735	9.596	**3.204**	3.923	15.524
	multi-FCNdAE	**3.768**	4.999	3.648	4.242	6.577
RMSE	dAE	147.845	17.951	59.814	43.969	126.089
	biLSTM	119.314	12.621	72.497	54.043	91.186
	FCNdAE	37.547	12.334	**37.887**	**33.759**	**40.075**
	U-Net	163.166	26.241	42.638	37.223	133.774
	multi-FCNdAE	**35.550**	**9.905**	41.138	44.936	45.464
EAC	dAE	0.703	0.879	0.789	0.786	0.425
	biLSTM	0.718	0.946	0.647	0.773	0.779
	FCNdAE	0.923	**0.946**	0.897	**0.880**	**0.930**
	U-Net	0.802	0.868	**0.913**	0.811	0.706
	multi-FCNdAE	**0.955**	0.931	0.901	0.796	0.876

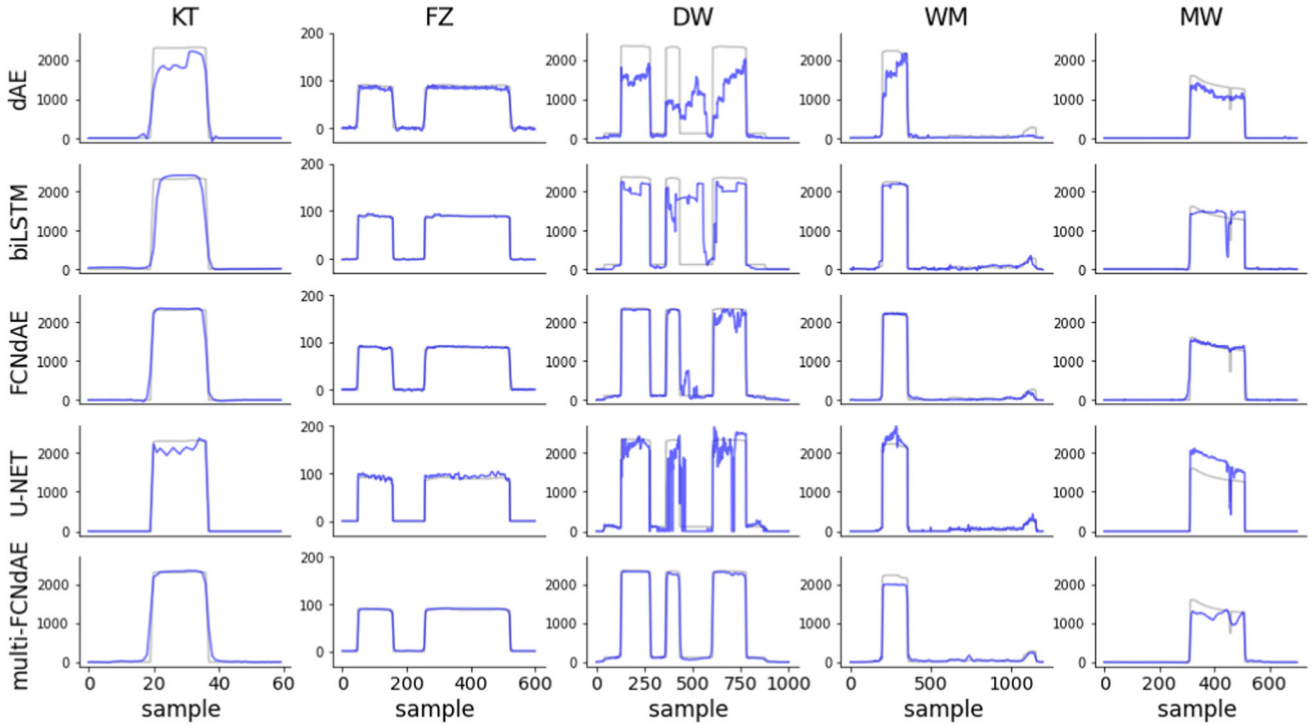

Fig. 4 Appliance consumptions from UK-DALE dataset (grey line) compared to their estimations (blue line) obtained from the dAE, biLSTM, FCNdAE, U-Net and multi-FCNdAE models

Figure 6a shows the number of trainable weights for multi-target architectures, and, in the case of single-target models, the sum of weights of all appliance-specific models $\{D_m\}$. It can be observed the invariance of the number of weights for the U-Net and biLSTM models to the change in the input length; while, the number of weights for the FCNdAE and multi-FCNdAE models varies with the input length. However, the multi-FCNdAE approaches require substantially fewer weights than the biLSTM and U-Net approaches for all input lengths. The output of the multi-target U-Net architecture relies on fully connected layers, which notably increases the number of weights in the model. Conversely, FiLM conditioning only introduces the weights of the FiLM generator.

Figure 6b denotes the time required by models to disaggregate a 5-hour sequence of main consumption **P**. For

Table 4 MAE and EAC metrics of the dAE, biLSTM, FCNdAE, multi-target U-Net and *multi-FCNdAE* approaches for the hospital dataset

		Data centre	Floors	Lifts	Rehab	X-ray
MAE	dAE	2.785	1.760	1.832	1.098	10.341
	biLSTM	2.701	1.912	2.372	1.135	6.676
	FCNdAE	0.999	1.285	1.695	0.768	4.097
	U-Net	0.851	2.501	3.188	1.330	4.766
	multi-FCNdAE	**0.300**	**1.135**	**1.540**	**0.703**	**3.045**
RMSE	dAE	3.373	2.304	2.620	1.509	13.569
	biLSTM	3.233	2.548	3.261	1.536	10.020
	FCNdAE	1.353	1.791	2.463	1.160	7.026
	U-Net	1.408	3.246	4.141	1.670	6.944
	multi-FCNdAE	**0.561**	**1.579**	**2.282**	**1.054**	**5.204**
EAC	dAE	0.975	0.972	0.974	0.973	0.824
	biLSTM	0.976	0.970	0.966	0.972	0.886
	FCNdAE	0.991	0.980	0.976	0.981	0.930
	U-Net	0.992	0.960	0.954	0.968	0.919
	multi-FCNdAE	**0.997**	**0.982**	**0.978**	**0.983**	**0.948**

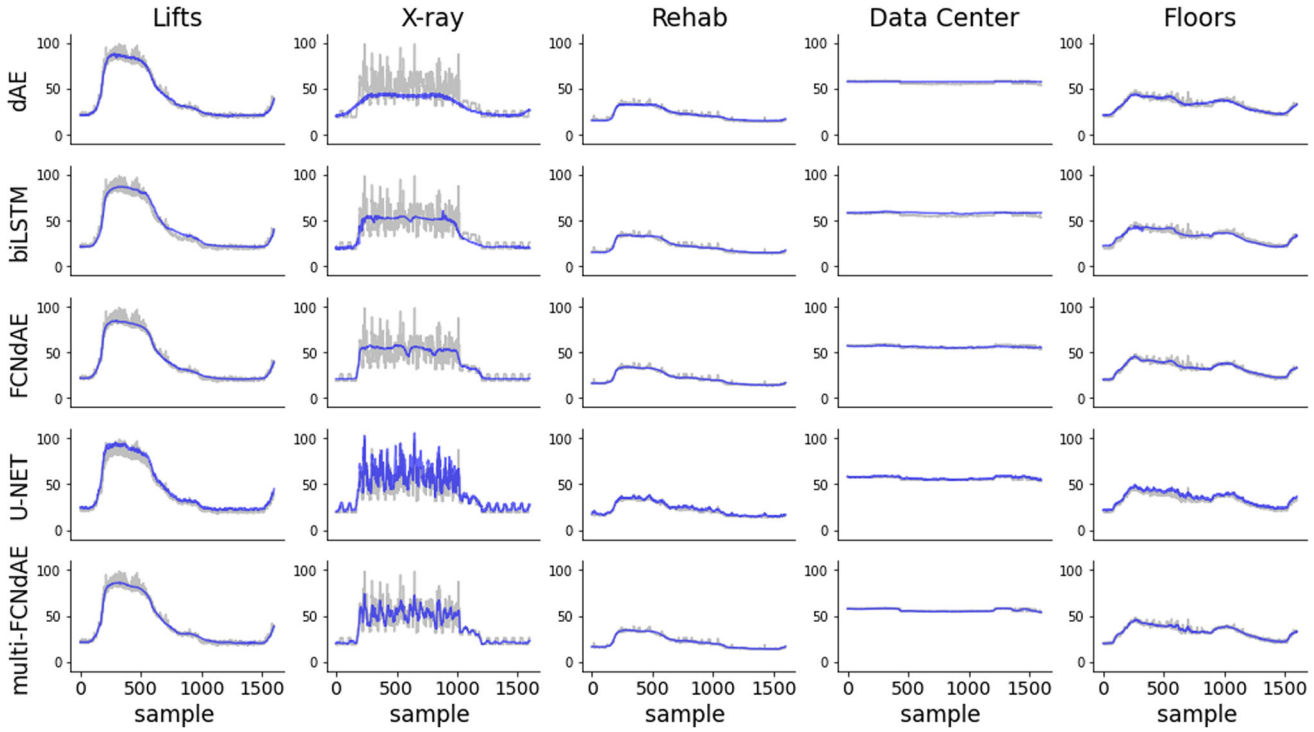

Fig. 5 Individual consumptions from hospital data (grey line) compared to their estimations (blue line) obtained from the dAE, biLSTM, FCNdAE, U-Net and multi-FCNdAE models

single-target methods, the displayed times comprise the execution of all the networks $\{D_m\}$ trained to predict the individual consumption corresponding to each appliance. It can be observed that the single-target FCNdAE approach is the fastest method for estimating the individual consumption sequences. The multi-FCNdAE model is slower than U-Net for short input sequences, but faster for long input sequences, and is comparable to standard FCNdAE models. The FiLM conditioning layers defined in (5) and the need to enter the input multiple times by varying the conditioning input $\mathbf{S}$ could delay the disaggregation process of the multi-target FiLM model.

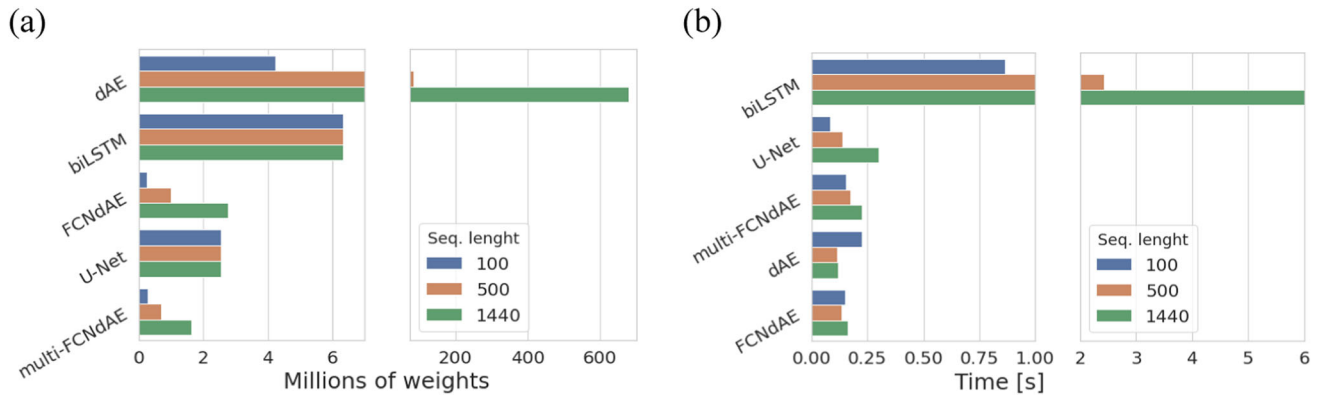

Fig. 6 Number of trainable weights (**a**) and inference time (**b**) computed for all the studied NILM methods for input sequences of 100, 500 and 1440 time steps

5.4 Interpretability opportunities of conditioned NILM

This section explores the possibilities of the conditioned NILM approach to improve the overall interpretability and user's confidence in the NILM model. Three strategies are proposed: 1) investigating the effects of FiLM in the latent space, 2) creating interpretable transitions between individual consumptions; and 3) exploiting the β and γ parameters to highlight relevant inner filters.

Effects of FiLM in the latent space. The multi-FCNdAE approach uses the FiLM conditioning method to adaptively modulate the encoder feature maps based on the targeted individual consumptions indicated in $\mathbf{S}$ by means of the $\mathbf{S}_m$ one-hot vectors. Thus, an input sequence $\mathbf{P}^{(i)}$ can be projected into different regions of the latent space depending on $\mathbf{S}_m$. This results in a latent space representation $\mathbf{z}_m^{(i)}$ conditioned on the selected m-th appliance.

Figure 7 shows the latent space representation of a set of input sequences $\mathbf{P}^{(i)}$ for both datasets. Each sequence $\mathbf{P}^{(i)}$ is processed N times (one per appliance), varying the input $\mathbf{S}_m$. The resulting $\mathbf{z}_m^{(i)}$ are then projected by the *Uniform Manifold Approximation and Projection* (UMAP) [38] to visualise a 2D map of the latent space. The UMAP view reveals that the FiLM transformations divide the latent space into appliance-specific regions. From these regions, the decoder reconstructs the individual target consumption. The location of node-specific clusters in the view also appears to be meaningful, since similar nodes are projected together, and those nodes that are different from each other are mapped apart. For instance, in the UK-DALE map, the latent space regions of the kettle and microwave are close to each other, since both devices have similar energy demand and ON durations (see Fig. 4). Likewise, in the hospital map the Data Centre area is significantly distant from the rest of the nodes, indicating its distinct nature (see Fig. 5).

Interaction with the conditioning input. FiLM transformations allow for continuous interaction with the conditioning input $\mathbf{S}_m$, enabling the end user to input

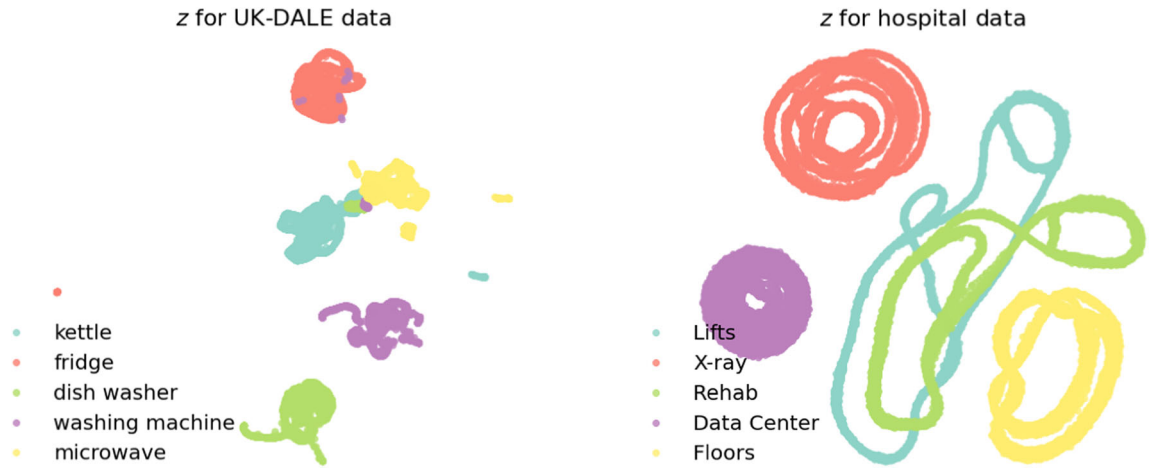

Fig. 7 UMAP projections of the conditioned latent space $\mathbf{z}_m$

trajectories in the appliance space and receive a transition between disaggregated nodes as output.

Figure 8 shows several examples of continuous transitions obtained after introducing the same window $\mathbf{P}^{(i)}$ into the model and several points of the trajectory $\mathbf{S} = (1 - \lambda)\mathbf{S}_{\text{app1}} + \lambda\mathbf{S}_{\text{app2}}$ between two appliances, varying λ in the range [0, 1]. These transitions insightfully reveal to the user which changes should be applied to the starting individual node to turn it into the end node. This idea is closely related to the field of *explainable machine learning*, especially with counterfactual examples [49], since the proposed model is able to reveal which learned features make two sequences from individual nodes different.

Relevant inner filters. The FiLM parameters in Eq. (5) provide information about the relevance of the convolution kernels according to the targeted individual consumption in $\mathbf{S}$. In particular, the scaling parameter $\gamma_{j,k}$ inhibits or promotes the k-th channel of the feature map $\mathbf{F}_{j,k}$ for the j-th convolution layer. As shown in Fig. 9, the user can simultaneously analyse the activation maps $\mathbf{F}_j$ and parameters γ_j values, to better understand the inner importance of each kernel in the inner computation of the network. The γ_j values improve the analysis of $\mathbf{F}_j$ compared to the standard multi-target models [16], where the feature maps cannot be contextualised with each output appliance. The interpretability of the feature map analysis in Fig. 9 is limited by the interactions between positive and negative values of $\mathbf{F}_j$ and γ_j, thereby complicating the association of the highlighted activations with recognisable patterns of the appliance selected by the one-hot vector $\mathbf{S}_m$. Although not covered in this article, imposing a non-negative constraint on the FiLM parameters potentially enhances the interpretability of the analysis in Fig. 9. However, it is important to note that this may penalise the overall accuracy of the system.

6 Conclusion

This article investigates the effectiveness of a multi-target NILM model, based on a Fully Convolutional denoising Autoencoder, denoted as multi-FCNdAE. The study concludes that:

- The proposed model predicts multiple individual consumptions using only one trained network, reducing the computational cost of the model, especially for large input sequences.
- The use of a conditioning input based on Feature-wise Linear Modulation (FiLM) technique allows specifying the target device. This input efficiently modulates intermediate convolution layers and enables the user to guide the model in an insightful way.
- Performance is evaluated in different scenarios such as residential buildings, using the well-known UK-DALE

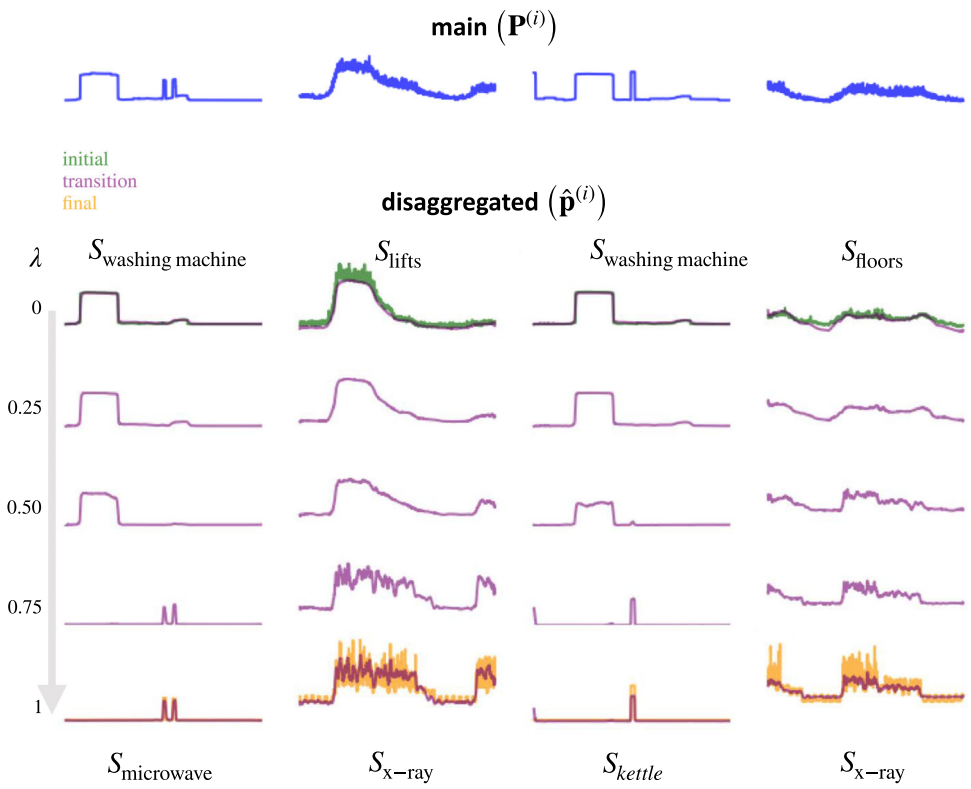

Fig. 8 Examples of transitions driven by the trajectory $\mathbf{S} = (1 - \lambda)\mathbf{S}_{\text{app1}} + \lambda\mathbf{S}_{\text{app2}}$ in the conditioning input. The transitions from the initial appliance in green ($\lambda = 0$) to the final appliance ($\lambda = 1$) in orange are represented by purple lines

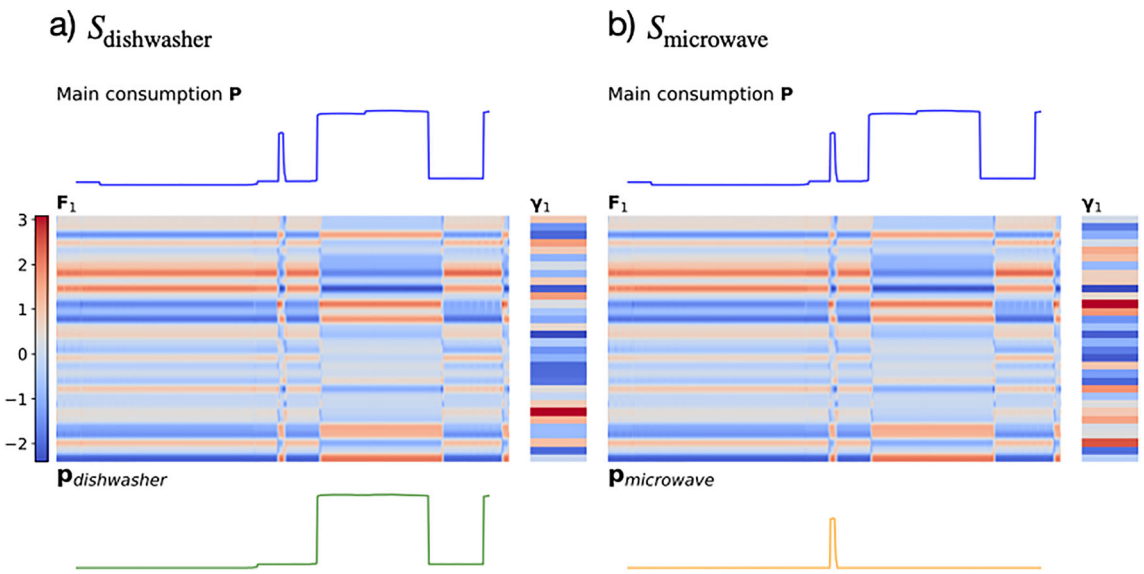

Fig. 9 Feature maps $\mathbf{F}_1$ of the first convolution layer and their corresponding γ_1 parameters. They are obtained from the same main sequence **P** (blue line) and using in **S** the one-hot vectors $\mathbf{S}_m$ for $m =$ dishwasher (**a**) and $m =$ microwave (**b**)

dataset, and in non-residential buildings using data from a hospital facility.

- A comparison is executed using both single-target and multi-target methods, revealing that the multi-FCNdAE model exhibits competitive accuracy when compared to single-target models, especially in non-residential contexts, and demonstrates improvement over a widely used multi-target approach.

The multi-FCNdAE technique is characterised by a minimal number of trainable weights, which reduces complexity and improves inference times. This enhances the model deployment in real-world facilities. The incorporation of the FiLM technique provides three different ways to better understand the model: conditioned latent space, continuous transitions between predicted individual consumptions and the analysis of the FiLM parameters. These provide valuable information about the inner mechanisms that drive the predictions of the model.

This work faces some limitations and challenges that are beyond the scope of this article and pave the way for future work. Firstly, the accuracy of multi-FCNdAE approaches is slightly outperformed by other single-target FCNdAE in some household appliances, owing to data variability and complexities in appliance usage patterns. Secondly, the interpretability of gamma weights is constrained by sign cancellations (see Sect. 5.4). Lastly, further experiments are necessary regarding the portability of the proposed model to new contexts. For instance, when an unseen individual consumption is connected.

Additional potential avenues for future research include extending the conditioning mechanism FiLM to other NILM methods, refining techniques to enhance inference times, and exploring knowledge integration and interpretability for more interactive user experiences. By addressing these aspects, the study lays the foundation for advancing NILM methodologies to make them more accessible, efficient, and user-friendly.

Acknowledgements This work was supported by the Ministerio de Ciencia e Innovación/Agencia Estatal de Investigación (MCIN/AEI/10.13039/501100011033) under grants PID2020- 115401GB-I00 and PID2020-117890RB-I00. Data were provided by Hospital of León and SUPPRESS Research Group of University of León within the project DPI2015- 69891-C2-1/2-R.

Funding Open Access funding provided thanks to the CRUE-CSIC agreement with Springer Nature.

Data availability The authors declare that the data supporting the findings of this study in a residential scenario are available. Supplementary information files and data can be found at 10.5286/UKERC.EDC.000004. Non-residential data from the hospital facility is not publicly available due to its strategic and private nature. The source code necessary to reproduce the results can be found at https://github.com/gsdpi/CondMultiTargetNILM.

References

1. Aboulian A, Green DH, Switzer JF et al (2018) NILM dashboard: a power system monitor for electromechanical equipment diagnostics. IEEE Trans Industr Inf 15(3):1405–1414
2. Aggarwal A (2020) Enhancement of gps position accuracy using machine vision and deep learning techniques. J Comput Sci 16(5):651–659
3. Altrabalsi H, Stankovic V, Liao J et al (2016) Low-complexity energy disaggregation using appliance load modelling. Aims Energy 4(1):884–905
4. Angelis GF, Timplalexis C, Krinidis S et al (2022) NILM applications: literature review of learning approaches, recent developments and challenges. Energy and Buildings
5. Barker S, Kalra S, Irwin D et al (2014) NILM redux: The case for emphasizing applications over accuracy. In: NILM-2014 workshop, Citeseer
6. Batic D, Stankovic V, Stankovic L (2023) Towards transparent load disaggregation–a framework for quantitative evaluation of explainability using explainable AI. IEEE Transactions on Consumer Electronics
7. Bonfigli R, Felicetti A, Principi E et al (2018) Denoising autoencoders for non-intrusive load monitoring: improvements and comparative evaluation. Energy and Buildings 158:1461–1474. https://doi.org/10.1016/j.enbuild.2017.11.054
8. Brewitt C, Goddard N (2018) Non-intrusive load monitoring with fully convolutional networks. arXiv preprint arXiv:1812.03915
9. Buddhahai B, Makonin S (2021) A nonintrusive load monitoring based on multi-target regression approach. IEEE Access 9:163033–163042
10. Chen K, Zhang Y, Wang Q et al (2019) Scale-and context-aware convolutional non-intrusive load monitoring. IEEE Trans Power Syst 35(3):2362–2373
11. Dhingra B, Liu H, Yang Z et al (2016) Gated-attention readers for text comprehension. arXiv preprint arXiv:1606.01549
12. Dumoulin V, Shlens J, Kudlur M (2016) A learned representation for artistic style. arXiv preprint arXiv:1610.07629
13. Dumoulin V, Perez E, Schucher N et al (2018) Feature-wise transformations. Distill https://doi.org/10.23915/distill.00011, https://distill.pub/2018/feature-wise-transformations
14. Ehrhardt-Martinez K, Donnelly KA, Laitner S et al (2010) Advanced metering initiatives and residential feedback programs: a meta-review for household electricity-saving opportunities. American Council for an Energy-Efficient Economy Washington, DC
15. Faustine A, Mvungi NH, Kaijage S et al (2017) A survey on non-intrusive load monitoring methodies and techniques for energy disaggregation problem. arXiv preprint arXiv:1703.00785
16. Faustine A, Pereira L, Bousbiat H et al (2020) Unet-nilm: A deep neural network for multi-tasks appliances state detection and power estimation in nilm. In: Proceedings of the 5th International Workshop on Non-Intrusive Load Monitoring, pp 84–88
17. Figueiredo M, De Almeida A, Ribeiro B (2012) Home electrical signal disaggregation for non-intrusive load monitoring (nilm) systems. Neurocomputing 96:66–73
18. Gans W, Alberini A, Longo A (2013) Smart meter devices and the effect of feedback on residential electricity consumption: evidence from a natural experiment in northern ireland. Energy Econ 36:729–743
19. García D, Díaz I, Pérez D et al (2018) Interactive visualization for NILM in large buildings using non-negative matrix factorization. Energy and Buildings 176:95–108
20. García D, Pérez D, Papapetrou P et al (2023) Conditioned fully convolutional denoising autoencoder for energy disaggregation. In: IFIP International Conference on Artificial Intelligence Applications and Innovations, Springer, pp 421–433
21. Garcia-Perez D, Perez-Lopez D, Diaz-Blanco I et al (2020) Fully-convolutional denoising auto-encoders for NILM in large non-residential buildings. IEEE Trans Smart Grid 12(3):2722–2731
22. Gopinath R, Kumar M, Joshua CPC et al (2020) Energy management using non-intrusive load monitoring techniques-state-of-the-art and future research directions. Sustain Cities Soc 62:102411
23. Harell A, Makonin S, Bajić IV (2019) Wavenilm: A causal neural network for power disaggregation from the complex power signal. ICASSP 2019–2019 IEEE International Conference on Acoustics. Speech and Signal Processing (ICASSP), IEEE, pp 8335–8339
24. Hart GW (1992) Nonintrusive appliance load monitoring. Proc IEEE 80(12):1870–1891
25. Hu J, Shen L, Sun G (2018) Squeeze-and-excitation networks. In: Proceedings of the IEEE conference on computer vision and pattern recognition, pp 7132–7141
26. Huber P, Calatroni A, Rumsch A et al (2021) Review on deep neural networks applied to low-frequency nilm. Energies 14(9):2390
27. Iqbal HK, Malik FH, Muhammad A et al (2021) A critical review of state-of-the-art non-intrusive load monitoring datasets. Electric Power Syst Res 192:106921
28. Kalinke F, Bielski P, Singh S et al (2021) An evaluation of nilm approaches on industrial energy-consumption data. In: Proceedings of the Twelfth ACM International Conference on Future Energy Systems, pp 239–243
29. Kaselimi M, Doulamis N, Voulodimos A et al (2020) Context aware energy disaggregation using adaptive bidirectional LSTM models. IEEE Trans Smart Grid 11(4):3054–3067
30. Kaselimi M, Protopapadakis E, Voulodimos A et al (2022) Towards trustworthy energy disaggregation: a review of challenges, methods, and perspectives for non-intrusive load monitoring. Sensors 22(15):5872
31. Kelly J, Knottenbelt W (2015) Neural nilm: Deep neural networks applied to energy disaggregation. In: Proceedings of the 2nd ACM International Conference on Embedded Systems for Energy-Efficient Built Environments, pp 55–64
32. Kelly J, Knottenbelt W (2015) The UK-DALE dataset, domestic appliance-level electricity demand and whole-house demand from five UK homes. Sci Data 2(1):1–14
33. Kim H, Marwah M, Arlitt M et al (2011) Unsupervised disaggregation of low frequency power measurements. In: Proceedings of the 2011 SIAM International Conference on Data Mining. SIAM, pp 747–758
34. Kolter JZ, Jaakkola T (2012) Approximate inference in additive factorial HMMs with application to energy disaggregation. In: Artificial intelligence and statistics, pp 1472–1482
35. Krystalakos O, Nalmpantis C, Vrakas D (2018) Sliding window approach for online energy disaggregation using artificial neural networks. In: Proceedings of the 10th Hellenic Conference on Artificial Intelligence, pp 1–6
36. LeCun Y, Bengio Y, Hinton G (2015) Deep learning. Nature 521(7553):436–444
37. Liao J, Elafoudi G, Stankovic L et al (2014) Non-intrusive appliance load monitoring using low-resolution smart meter data. In: 2014 IEEE International Conference on Smart Grid Communications (SmartGridComm), IEEE, pp 535–540
38. McInnes L, Healy J, Melville J (2018) Umap: Uniform manifold approximation and projection for dimension reduction. arXiv preprint arXiv:1802.03426
39. Mirza M, Osindero S (2014) Conditional generative adversarial nets. arXiv preprint arXiv:1411.1784

40. Moradzadeh A, Mohammadi-Ivatloo B, Abapour M et al (2021) A practical solution based on convolutional neural network for non-intrusive load monitoring. J Ambient Intell Humaniz Comput 12:9775–9789
41. Murray D, Stankovic L, Stankovic V (2020) Explainable nilm networks. In: Proceedings of the 5th International Workshop on non-intrusive load monitoring, pp 64–69
42. do Nascimento PPM (2016) Applications of deep learning techniques on NILM. Diss Universidade Federal do Rio de Janeiro
43. Oord Avd, Dieleman S, Zen H et al (2016) Wavenet: A generative model for raw audio. arXiv preprint arXiv:1609.03499
44. Pereira L, Nunes N (2018) Performance evaluation in non-intrusive load monitoring: datasets, metrics, and tools-a review. Wiley Interdiscip Rev Data Min Knowl Disc 8(6):e1265
45. Perez E, Strub F, De Vries H et al (2018) Film: Visual reasoning with a general conditioning layer. In: Thirty-Second AAAI Conference on Artificial Intelligence
46. Schirmer PA, Mporas I (2022) Non-Intrusive Load Monitoring: A Review. IEEE Trans Smart Grid 14(1):769–784
47. Shin C, Joo S, Yim J et al (2019) Subtask gated networks for non-intrusive load monitoring. In: Proceedings of the AAAI Conference on Artificial Intelligence, pp 1150–1157
48. Völker B, Pfeifer M, Scholl PM et al (2020) A Versatile High Frequency Electricity Monitoring Framework for Our Future Connected Home. In: Sustainable Energy for Smart Cities: First EAI International Conference, SESC 2019, Braga, Portugal, December 4–6, 2019, Proceedings 1, Springer, pp 221–231
49. Wang Z, Samsten I, Mochaourab R et al (2021) Learning Time Series Counterfactuals via Latent Space Representations. In: Discovery Science: 24th International Conference, DS 2021, Halifax, NS, Canada, October 11–13, 2021, Proceedings 24, Springer, pp 369–384
50. Yang Y, Zhong J, Li W et al (2019) Semisupervised multilabel deep learning based nonintrusive load monitoring in smart grids. IEEE Trans Industr Inf 16(11):6892–6902
51. Zhang C, Zhong M, Wang Z et al (2018) Sequence-to-point learning with neural networks for non-intrusive load monitoring. In: Thirty-second AAAI conference on artificial intelligence
52. Zhang Y, Yang G, Ma S (2019) Non-intrusive load monitoring based on convolutional neural network with differential input. Procedia CIRP 83:670–674. https://doi.org/10.1016/j.procir.2019.04.110, https://www.sciencedirect.com/science/article/pii/S2212827119307243, 11th CIRP Conference on Industrial Product-Service Systems
53. Zhuang M, Shahidehpour M, Li Z (2018) An overview of non-intrusive load monitoring: Approaches, business applications, and challenges. In: 2018 International Conference on Power System Technology (POWERCON), IEEE, pp 4291–4299
54. Zoha A, Gluhak A, Imran MA et al (2012) Non-intrusive load monitoring approaches for disaggregated energy sensing: a survey. Sensors 12(12):16838–16866